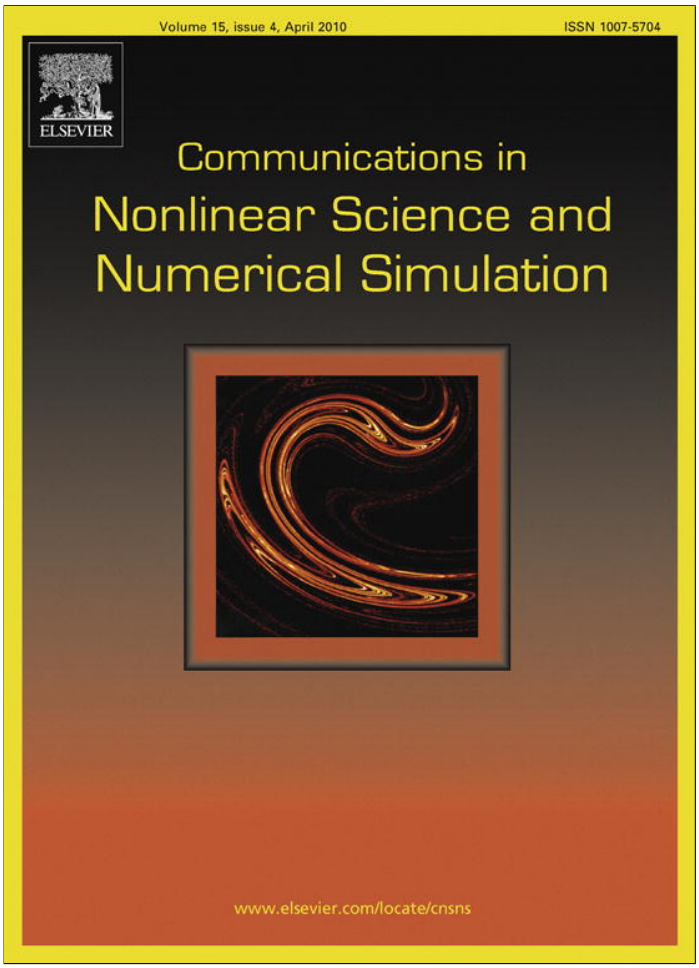

Commun Nonlinear Sci Numer Simulat 15 (2010) 869–880

Contents lists available at ScienceDirect

Commun Nonlinear Sci Numer Simulat

journal homepage: www.elsevier.com/locate/cnsns

Radius of analyticity and exponential convergence for spectral projections of the generalized KdV equation

Magnar Bjørkavåg, Henrik Kalisch *

Department of Mathematics, University of Bergen, Johannes Brunsgate 12, 5008 Bergen, Norway

ARTICLE INFO

Article history:
Received 24 November 2008
Received in revised form 5 April 2009
Accepted 5 May 2009
Available online 12 May 2009

PACS:
02.30.Jr
02.70.Hm
47.35.Fg

Keywords:
Generalized Korteweg–de Vries equation
Radius of analyticity
Fourier–Galerkin method
Spectral convergence

ABSTRACT

In this paper an exponential convergence rate for a spectral projection of the periodic initial-value problem for the generalized KdV equation is proved. Based on this convergence result, a method for determining the radius of analyticity of solutions of the generalized KdV equation is derived. Results from the new method and a similar method are compared.

1. Introduction

Consideration is given to real-valued solutions of the generalized Korteweg–de Vries (gKdV) equation

$$\partial_t u + \frac{1}{p}\partial_x(u^p) + \partial_x^3 u = 0, \tag{1.1}$$

where p denotes an integer greater than or equal to 2. The cases $p = 2$ and $p = 3$ are especially pertinent when it comes to applications, as these equations appear as models for surface water waves, and are also used in a variety of other modeling situations [9,11].

Much of the recent work on (1.1) has focused on low-regularity solutions [6,8,19]. However, there have also been studies aimed at understanding solutions with high regularity. It is known that (1.1) admits real-analytic solutions for all $p \geqslant 2$ [5,14,18]. In particular, if initial data are given which extend analytically to a strip about the real axis and satisfy some mild integrability conditions, then it may be shown that the solution can also be extended analytically to a possibly smaller strip as long as the solution exists. The width of this strip is commonly called the *radius of analyticity*. Precise estimates for the radius of analyticity have been given in [14].

Here we explore connections between the radius of analyticity and convergence properties of spectral projections of (1.1). For the gKdV equation with *quadratic* nonlinearity, the convergence of spectral projections was proved by Maday and Quarteroni in [20]. In particular, they showed that for smooth solutions $u(x,t)$ so-called spectral convergence is achieved. That is,

* Corresponding author.
E-mail addresses: magnar.bjorkavag@math.uib.no (M. Bjørkavåg), henrik.kalisch@math.uib.no (H. Kalisch).

1007-5704/$ - see front matter © 2009 Elsevier B.V. All rights reserved.
doi:10.1016/j.cnsns.2009.05.015

for the difference between a smooth solution u and the spectral approximation u_N with N Fourier modes on some time interval $[0,T]$, the estimate

$$\sup_{t\in[0,T]} \|u(\cdot,t) - u_N(\cdot,t)\| \leqslant \Lambda_T N^{-m} \tag{1.2}$$

holds for any m.

In the case $p = 2$, it was shown in [2,15] that the convergence rate is actually exponential if u is analytic in a strip about the real axis. In the present paper, we generalize this result to any $p \geqslant 2$. Thus if u denotes a real-valued solution of (1.1) which is analytic on a strip of width 2σ about the real axis, and u_N denotes the solution of a (semi-discrete) Fourier–Galerkin approximation of (1.1) on a time interval $[0,T]$, then we prove the estimate

$$\sup_{t\in[0,T]} \|u(\cdot,t) - u_N(\cdot,t)\| \leqslant \Lambda N e^{-\sigma N}, \tag{1.3}$$

for some positive constant Λ. To illustrate the significance of the improvement of the exponential convergence estimate (1.3) over the standard spectral estimate (1.2), a smooth but non-analytic solution has to be found. This is not in general easy (cf. [13]). Here, we use the inhomogeneous KdV equation

$$\partial_t u + u\partial_x u + \partial_x^3 u = f.$$

For an appropriate choice of f, this equation has solutions known in exact form. First, the function $u(x,t) = e^{-\frac{1}{\sin^2(x-t)}}$ is used as the exact solution. Note that this function is smooth, but not real-analytic. The values shown as boxes in Fig. 1 are the L^2-error between the exact solution u and the computed approximation u_N. For this function, spectral convergence is achieved. Next, we use the function $u(x,t) = \frac{1}{1+\sin^2(x-t)}$ which is analytic for complex values of x with imaginary part no larger than $\pi/2$. The resulting L^2-errors are shown as circles in Fig. 1. Finally, convergence of a finite-difference discretization of the analytic solution is indicated with diamonds. From Fig. 1, it strikingly appears that the advantage of traditional spectral convergence over the finite-difference method pales in comparison with the exponential convergence which is achieved if analytic solutions are approximated. Thus with a view towards computational efficiency, it can be important to have available the exponential convergence estimate proved in this paper. Our work is organized as follows. In the remainder of the introduction, relevant mathematical notation and some auxiliary estimates are established. Then, in Section 2, the spectral projection is defined and the exponential convergence estimate proved. Some computational issues and a method for estimating σ are presented in Section 3. The technique under review is also compared to a method advocated by Sulem, Sulem and Frisch [23]. Both methods are then used to find σ as a function of time for general initial data in Section 4. Finally, a numerical experiment is set up to see how σ behaves in time for a solution which experiences blow-up in finite time.

The results in this article hold for 2π-periodic real-valued solutions of (1.1) which are real analytic functions in the spatial variable x. To quantify the domain of analyticity, the class of periodic analytic Gevrey spaces are introduced. These are given by the norm

$$\|f\|_{G_\sigma}^2 = \sum_{k\in\mathbb{Z}} e^{2\sigma\sqrt{1+|k|^2}} \left|\hat{f}(k)\right|^2,$$

for some $\sigma > 0$. Here $\hat{f}(k)$ are the Fourier coefficients of a 2π periodic function f. To enforce that these functions restrict to real-valued functions on the real line, the relation $\hat{f}(-k) = \overline{\hat{f}(k)}$ is used for the Fourier coefficients.

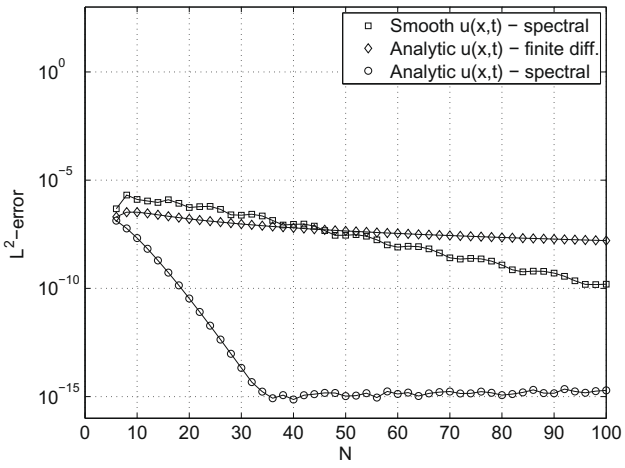

Fig. 1. It appears that the exponential convergence rate which holds for analytic solutions is more advantageous than both the traditional spectral convergence and the algebraic convergence of a finite-difference scheme.

The usual periodic Sobolev spaces are given by the norm

$$\|f\|_{H^s}^2 = \sum_{k\in\mathbb{Z}} (1+|k|^2)^s \left|\hat{f}(k)\right|^2,$$

and for $s=0$, the space $H^0(0,2\pi) = L^2(0,2\pi)$ appears. We will also have occasion to consider the mixed Sobolev-Gevrey norms

$$\|f\|_{G_{\sigma,s}} = \sum_{k\in\mathbb{Z}} (1+|k|^2)^s e^{2\sigma\sqrt{1+|k|^2}} \left|\hat{f}(k)\right|^2.$$

The L^2-norm will for simplicity be denoted by $\|\cdot\|$, and the inner product on this space is given by

$$(f,g) = \int_0^{2\pi} f(x)\overline{g(x)}\,dx.$$

Finally, we will need the Sobolev inequality

$$\sup_x |f(x)| \leqslant C\|f\|_{H^1}, \tag{1.4}$$

for functions $f \in H^1$. In order to define the spectral projection, a finite dimensional subspace S_N of $L^2(0,2\pi)$ is introduced. It is defined as

$$S_N = \operatorname{span}_{\mathbb{C}}\{e^{ikx} | k\in\mathbb{Z}, -N\leqslant k\leqslant N\}.$$

The operator P_N denotes the orthogonal projection from $L^2(0,2\pi)$ onto S_N, and is defined by

$$P_N f(x) = \sum_{-N\leqslant k\leqslant N} e^{ikx}\hat{f}(k).$$

The operator P_N may also be characterized by the property that, for any $f\in L^2(0,2\pi)$, $P_N f$ is the unique element in S_N such that

$$(P_N f,\phi) = (f,\phi), \tag{1.5}$$

for all $\phi\in S_N$. Furthermore, for $r\geqslant 0$ and $\sigma>0$, the estimate

$$\|f-P_N f\|_{H^r} \leqslant N^r e^{-\sigma N}\|f\|_{G_\sigma}, \tag{1.6}$$

is obtained by a straightforward calculation. Finally, note the inverse inequality (see [7])

$$\left\|\partial_x^m \phi\right\| \leqslant N^m \|\phi\|, \tag{1.7}$$

which holds for integers $m>0$ and functions $\phi\in S_N$.

2. The spectral projection

To obtain a well posed problem, Eq. (1.1) has to be supplemented with appropriate boundary and initial conditions. For the numerical approximation, the problem will be studied on a finite interval with periodic boundary conditions. The periodic initial value problem for (1.1) is

$$\begin{cases} \partial_t u + \frac{1}{p}\partial_x(u^p) + \partial_x^3 u = 0, & x\in[0,2\pi], \quad t\geqslant 0,\\ u(0,t) = u(2\pi,t), & t\geqslant 0,\\ u(x,0) = u_0(x), \end{cases} \tag{2.1}$$

In the following, it will be assumed that a solution of this problem exists on some time interval $[0,T]$ and with a certain amount of spatial regularity. In particular, we suppose that a solution exists in the space $C([0,T],G_\sigma)$ for some $\sigma>0$ and $T>0$. For analytic initial data, there are a number of results guaranteeing the existence of solutions in the Gevrey space G_σ [4,17,18]. In general, for $p<5$, the well posedness is global in time, while for $p\geqslant 5$, the solution may only exist for a short time. Since the existence of a solution in the Sobolev spaces H^s is well understood [8], the critical question is only the Gevrey regularity. The following theorem was proved in [17].

Theorem 2.1. *Suppose that $u\in C([0,T],H^s)$ is a solution of (2.1) with $p=2$, with initial data $u_0\in G_{\sigma_0,s}$ for some $\sigma_0>0$ and $s>\frac{5}{2}$. Then $u(\cdot,t)$ extends uniquely to a function in $G_{\sigma(t),s}$ with $\sigma(t)$ given by*

$$\sigma(t) = \sigma_0 e^{-ct\|u_0\|_{G_{\sigma_0,s}}} e^{-ct^{3/2}},$$

for some constant c independent of t. Moreover, for any $\tau\in(0,T]$, we have $u\in C([0,\tau],G_{\sigma(\tau),s})$, and the estimate

$$\|u(\cdot,t)\|_{G_{\sigma(\tau),s}} \leqslant \|u_0\|_{G_{\sigma_0,s}} + c\sqrt{t},$$

holds for another constant c independent of t.

A similar theorem can be proved for $p = 3$ and $p = 4$, using the estimates in [4]. For $p \geqslant 5$, a similar result is also available if it is assumed that the solution does not blow up on the time interval $[0, T]$. Finally, note that we have the estimate

$$\|u_0\|_{G_{\sigma-\varepsilon,s}} \leqslant c_{s,\varepsilon}\|u_0\|_{G_\sigma}$$

for any $\varepsilon > 0$ and any $\sigma > 0$ and $s > 0$ [5]. This shows that the Sobolev weight in the $G_{s,\sigma}$-norm is inconsequential when considering the radius of analyticity.

The Galerkin approximation to (2.1) is given by a function u_N from $[0, T]$ to S_N satisfying

$$\begin{cases} \left(\partial_t u_N + \frac{1}{p}\partial_x(u_N^p) + \partial_x^3 u_N, \phi\right) = 0, \quad t \in [0, T], \\ u_N(x, 0) = P_N u_0(x), \end{cases} \tag{2.2}$$

for all $\phi \in S_N$. Since for each $t, u_N(\cdot, t) \in S_N$, the approximation u_N has the form

$$u_N(x, t) = \sum_{k=-N}^{N} \hat{u}_N(k, t)\, e^{ikx},$$

where $\hat{u}_N(k, t)$ are the Fourier coefficients of $u_N(\cdot, t)$. In particular, we have

$$u_N(x, 0) = \sum_{k=-N}^{N} \hat{u}_0(k)\, e^{ikx}. \tag{2.3}$$

Short time existence of a maximal solution of (2.2) is proved using the contraction mapping principle, and the solution is unique on its maximal interval of definition, $[0, t_N^m)$, where t_N^m is possibly equal to T. It can be seen that this solution is real-valued as follows. Taking the complex conjugate of each term in (2.2), it appears that $\overline{u_N}$ is a solution of (2.2) if u_N is. Eq. (2.3) shows that the initial data $u_N(\cdot, 0)$ is real if u_0 is real-valued. Since the solution u_N is unique, we have that $\overline{u_N} = u_N$.

The main result in this section is that the approximation u_N converges exponentially fast towards the solution u of (2.1) under certain assumptions on the regularity of this solution.

Theorem 2.2. *Suppose a solution u of (2.1) exists in the space $C([0, T], G_\sigma)$ for some $\sigma > 0$ and $T > 0$. Then, for N big enough, there exists a unique solution u_N of (2.2). Moreover, there exists a constant Λ such that*

$$\sup_{t\in[0,T]} \|u(\cdot, t) - u_N(\cdot, t)\| \leqslant \Lambda N e^{-\sigma N}.$$

Note that from the assumptions of Theorem 2.2 there exists constants κ and λ such that

$$\sup_{t\in[0,T]} \|u(\cdot, t)\|_{G_\sigma} \leqslant \kappa, \tag{2.4}$$

and

$$\sup_{t\in[0,T]} \|u(\cdot, t)\|_{H^2} \leqslant \lambda. \tag{2.5}$$

Now a proof of convergence of solutions of the semi-discrete equation to a solution of (2.1) could proceed by combining a local convergence result with a stability result for some Sobolev norm. However, as it turns out, in order to prove the local convergence estimate in the following lemma, one needs stability of the H^2-norm of the discrete solution. For the cases $p = 2$ and $p = 3$, an infinite number of conserved integrals exist, and one might think to use discrete versions of these integrals in order to obtain stability of the H^2-norm. For $p = 2$, such an analysis has been carried out in [20]. However, for $p > 3$, no such conserved integrals exist, and one must devise an alternative approach. Here, we use a device which was already implicit in the work [20], and which has been used in [16]. Essentially, the exponential convergence rate is exploited to avoid the need of a stability result. First, let us prove local-in-time convergence under the assumption of stability.

Lemma 2.3. *Suppose that a solution u_N of (2.2) exists on the time interval $[0, t_N^*]$ and that $\sup_{t\in[0,t_N^*]}\|u_N(\cdot, t)\|_{H^2} \leqslant 2\lambda$. Then the error estimate*

$$\sup_{t\in[0,t_N^*]} \|u(\cdot, t) - u_N(\cdot, t)\| \leqslant \Lambda N e^{-\sigma N}$$

holds for some Λ, which only depends on t_N^*, and κ and λ as defined in (2.4) and (2.5).

Proof. To prove the local error estimate, consider the function $h = P_N u - u_N \in S_N$ as the test function in (2.2). Apply the projection operator P_N to (2.1), and subtract the spectral projection (2.2), to get

$$(\partial_t h, h) + \frac{1}{p}\left(\partial_x P_N(u^p) - \partial_x(u_N^p), h\right) + (\partial_x^3 h, h) = 0.$$

Since the third derivative operator is skew-symmetric, and all functions are real-valued, the last term is zero. Then the equation can be rewritten as

$$\frac{p}{2}\frac{d}{dt}\|h\|^2 = (P_N(u^p) - u^p, h_x) + \left(u^p - (P_N u)^p, h_x\right) + \left((P_N u)^p - u_N^p, h_x\right).$$

It follows from (1.5) that the first term appearing on the right-hand side is zero, since P_N is the orthogonal projection onto S_N. Therefore, for general p, the equation

$$\frac{p}{2}\frac{d}{dt}\|h\|^2 = \left(u^p - (P_N u)^p, h_x\right) + \left((P_N u)^p - u_N^p, h_x\right). \tag{2.6}$$

appears. For the sake of clarity, we will now treat the special case $p = 4$. The proof is easily modified to cover all other values of p. When $p = 4$ the first term in (2.6) can be written as

$$\begin{aligned}\left|\left(\partial_x(u^4 - (P_N u)^4), h\right)\right| \leqslant{}& \sup_x |(u + P_N u)(u^2 + (P_N u)^2)|\|\partial_x(u - P_N u)\|\|h\| + \sup_x |(u^2 + (P_N u)^2)\partial_x(u + P_N u)|\|u - P_N u\|\|h\| \\ &+ \sup_x |(u + P_N u)\partial_x(u^2 + (P_N u)^2)|\|u - P_N u\|\|h\|.\end{aligned}$$

From the Sobolev inequality (1.4) and (1.6), the estimate

$$\left|\left(\partial_x(u^4 - (P_N u)^4), h\right)\right| \leqslant 4C^3\|h\|\left(\|u\|_{H^1}^3\|u - P_N u\|_{H^1} + 3\|u\|_{H^2}^3\|u - P_N u\|\right) \leqslant 16C^3\lambda^3 N e^{-\sigma N}\|h\|\|u\|_{G_\sigma}$$

is derived. After one integration by parts, it is seen that the second term in (2.6) is bounded by

$$|((P_N u)^4 - u_N^4, h_x)| \leqslant \sup_x |\partial_x((P_N u + u_N)((P_N u)^2 + u_N^2))|\frac{1}{2}\|h\|^2.$$

Again, by employing (1.4) and (1.6), the estimate

$$\begin{aligned}|((P_N u)^4 - u_N^4, h_x)| &\leqslant \frac{C^3}{2}\|h\|^2\|P_N u + u_N\|_{H^2}\left(\|P_N u\|_{H^1}^2 + \|u_N\|_{H^1}^2\right) + \frac{C^3}{2}\|h\|^2\|P_N u + u_N\|_{H^1}\left(\|P_N u\|_{H^2}^2 + \|u_N\|_{H^2}^2\right) \\ &\leqslant \frac{45}{2}C^3\lambda^3\|h\|^2\end{aligned}$$

appears. Adding the contributions then gives

$$\frac{d}{dt}\|h\| \leqslant 4C^3\lambda^3\kappa N e^{-\sigma N} + \frac{45}{8}C^3\lambda^3\|h\|.$$

Using Gronwall's lemma, gives

$$\|h\| \leqslant 4C^3\lambda^3\kappa t_N^* e^{45C^3\lambda^3 t_N^*/8} N e^{-\sigma N} + \|h(\cdot,0)\|e^{45C^3\lambda^3 t_N^*/8}.$$

From the fact that $h(\cdot,0) = 0$ and using the triangle inequality, the following estimate appears

$$\|u - u_N\| \leqslant \|u - P_N u\| + \|h\| \leqslant \Lambda N e^{-\sigma N},$$

where

$$\Lambda = \kappa + 4C^3\lambda^3\kappa t_N^* e^{45C^3\lambda^3 t_N^*/8}. \tag{2.7}$$

Taking the supremum over t concludes the proof of the lemma. □

Lemma 2.3 provides an estimate for the L^2-norm of the error. However, in order to extend the previous local estimate to the time interval $[0, T]$, we need to know that the H^2-norm of u_N is bounded. The first step to achieving such a bound is to relate Lemma 2.3 to an estimate for the H^2-norm of the error.

Lemma 2.4. *Suppose that a solution u_N of (2.2) exists on the time interval $[0, t_N^*]$ and with $\sup_{t\in[0,t_N^*]}\|u(\cdot,t)\|_{H^2} \leqslant 2\lambda$. Then the error estimate*

$$\sup_{t\in[0,t_N^*]}\|u(\cdot,t) - u_N(\cdot,t)\|_{H^2} \leqslant \Lambda N^3 e^{-\sigma N}$$

holds for some Λ which only depends on t_N^*, and on κ and λ as defined in (2.4) and (2.5).

This lemma is deduced from the triangle inequality and the inverse inequality (1.7), after using the results from Lemma 2.3.

Proof of Theorem 2.2. The proof will be achieved if the time t_N^*, which has not been specified in Lemma 2.3, can be shown to be equal to T. First note that the constant Λ appearing in Lemmas 2.3 and 2.4 can be made independent of t_N^* by choosing T instead of t_N^* in the definition of Λ in (2.7). Now according to the statement of Lemma 2.3, t_N^* should be defined as the largest time in $[0, T]$ for which the H^2-norm of u_N is uniformly bounded by 2λ. That is,

$$t_N^* = \sup\left\{t \in [0,T] |\text{ for all } t' \leqslant t, \|u(\cdot,t')\|_{H^2} \leqslant 2\lambda\right\}.$$

It is clear that t_N^* is smaller than the maximal time of existence t_N^m. And also, from the definition, that it is either equal to T or smaller than T. In the latter case, since the H^2-norm of u_N is a continuous function in time, it follows that $\|u_N(\cdot,t_N^*)\|_{H^2} = 2\lambda$. And also, since $\|u_N(\cdot,0)\|_{H^2} = \|P_N u(\cdot,0)\|_{H^2}$, it follows that

$$\|u_N(\cdot,0)\|_{H^2} \leqslant \|u(\cdot,0)\|_{H^2} \leqslant \lambda,$$

and therefore $t_N^* > 0$ for all N.

While it is not possible that $t_N^* = T$ for all N, we will now aim to show the existence of a N^*, such that

$$t_N^* = T, \quad \text{for all} \quad N \geqslant N^*,$$

in which case the supremum in Lemma 2.3 extends to the interval $[0,T]$. Suppose then that $t_N^* < T$. Use the triangle inequality to get

$$2\lambda = \left\|u_N(\cdot,t_N^*)\right\|_{H^2} \leqslant \left\|u_N(\cdot,t_N^*) - u(\cdot,t_N^*)\right\|_{H^2} + \left\|u(\cdot,t_N^*)\right\|_{H^2} \leqslant \left\|u_N(\cdot,t_N^*) - u(\cdot,t_N^*)\right\|_{H^2} + \lambda,$$

from the definition of λ. Hence,

$$\lambda \leqslant \left\|u(\cdot,t_N^*) - u_N(\cdot,t_N^*)\right\|_{H^2}.$$

By Lemma 2.4 it follows that

$$\lambda \leqslant \Lambda N^3 e^{-\sigma N},$$

or

$$\frac{\lambda}{\Lambda} \leqslant N^3 e^{-\sigma N}.$$

So, from this it is clear that by choosing N large enough, the above inequality will not hold, and we must have $t_N^* = T$. □

3. Computational considerations

The purpose of this section is twofold. First, we want to use a known solution to confirm the results of the last section concerning the rate of convergence of the spectral projection of (1.1). Secondly, we want to test and compare two numerical methods for determining the radius of analyticity σ of an unknown solution of (1.1). Since we use solitary waves on the infinite line as exact solutions, it will be convenient to use the equation

$$\partial_t u + \frac{1}{p}\partial_x(u^p) + \frac{1}{a^3}\partial_x^3 u = 0, \tag{3.1}$$

instead of (1.1). Note that if the equation is considered on the real line, then a can be taken to be equal to one, as it disappears under the scaling $v(x,t) = a^{1/p-1}u(x/a,t)$. The significance of the parameter a in the periodic setting will become transparent presently.

Recall that (3.1) has special solutions known as solitary waves which are given explicitly by

$$\Phi_p(x) = A\sec h^{\frac{2}{p-1}}(\kappa a x) \quad \text{where} \quad \kappa = (p-1)\left(\frac{aA^{p-1}}{2p(p+1)}\right)^{1/2}. \tag{3.2}$$

These solutions of (3.1) are given on the whole real line. But if a is sufficiently large, they may be considered as a good approximation to solutions corresponding to periodic boundary conditions since the tails of these solutions decay exponentially and are zero to machine precision within the computational domain. Note also that the solitary waves are members of the space G_σ over $\mathbb{R}$ so long as $\sigma < \frac{\pi}{2\kappa a}$. This can easily be seen from locating the pole closest to the real line for the hyperbolic secant function.

We now turn to the problem of finding σ from numerical computations. To illustrate the two numerical methods for determining a possibly unknown radius of analyticity σ, the case $p = 2$ is used. For this solution the expression for the Fourier transform (FT)

$$\widehat{\Phi}_2(k) = \frac{A\pi k}{2\kappa a}\operatorname{csch}\left(\frac{\pi k}{2\kappa a}\right) \tag{3.3}$$

will be found useful. One straightforward approach is to estimate σ from the decay of the Fourier spectrum. This approach has been used by Sulem, Sulem and Frisch in [23]. A slightly more involved approach is to use the convergence rate of the numerical method to find σ. The centerpiece of the analysis here is given by a robust way of computing the error committed by the Galerkin projection. Thus for fixed N, we want to approximate the integral

$$\left\{\int_0^{2\pi} |u(x,t) - u_N(x,t)|^2\,dx\right\}^{1/2}.$$

While the convergence estimate in the previous section was given in terms of this integral one must resort to a numerical approximation of the above integral in practical computations. The approximation of the integral is often done on the grid used to obtain the numerical solution. That is, using a resolution N corresponding to a grid spacing $h_N = \frac{2\pi}{N}$, the L^2-error, E_D, is usually defined as

$$E_D^2(N) = h_N \sum_{j=1}^{N} |u(x_j,t) - u_N(x_j,t)|^2.$$

A problem with this definition is that both the error from the numerical method and the error from the approximation of the integral enter into the formula. However, one really wants to remove (to machine precision) or keep constant the part of E_D which is not due to the numerical projection of the differential equation. One way to achieve this is the use of an alternative definition of the L^2-error E_F, namely

$$E_F^2(N) = h_M \sum_{j=1}^{M} |u(x_j,t) - u_N^M(x_j,t)|^2$$

where $h_M = \frac{2\pi}{M}$, is constant for fixed $M \gg N$. For this to work, a way to find the discrete solution on the fine grid with M points, $u_N^M(x_j,t)$, $j = 1,2,\ldots,M$, is required. Generally, an interpolation routine of at least the same order as the numerical method has to be used. From the expansion coefficients $\hat{u}_N(k,t)$, an expression for u_N^M is easily found as

$$u_N^M(x_j,t) = \sum_{k=-N}^{N} \hat{u}_N(k,t) e^{ikx_j}, \quad j = 1,2,\ldots,M.$$

While the difference between using E_D and E_F appears unimportant when validating the convergence of a numerical implementation, the second definition is by far superior in determining the radius of analyticity σ from the convergence rate.

To illuminate the difference between using E_D or E_F, we will estimate σ from the L^2-errors for the case $p = 2$ as mentioned above. The estimates are based on the convergence results of the Galerkin projection and follows from assuming that the L^2-errors are of the form $\Lambda N e^{-\sigma N}$. A linear (in Λ and σ) least squares problem is constructed from this assumed form as

$$\log\left(\frac{E_{D/F}(N)}{N}\right) = \log(\Lambda) + (-\sigma)N.$$

The resulting overdetermined system is solved for $\log(\Lambda)$ and σ by a standard approach like QR-factorization or SVD. For graphical illustration, estimates of σ also follow from two consecutive L^2-errors as

$$\sigma = \frac{\log(E_{D/F}(N_1)/E_{D/F}(N_2)) - \log(N_1/N_2)}{(N_2 - N_1)}. \tag{3.4}$$

A plot of the L^2-errors E_D and E_F divided by N after 10 time steps is given in Fig. 2 (left) for $a = 34.2$ and $\kappa = 0.5$. With the linear-log axes used here, these quantities should appear linear with slopes equal to σ. Superimposed with a solid line in Fig. 2 (left) is a curve with a slope equal to the theoretical value of σ for comparison. It is seen that even though the magnitude of the errors E_D is smaller then E_F, the slope for the latter is closer to the slope of the superimposed curve. This is evident in Fig. 2 (right), where estimates of σ based on E_D and E_F are plotted using (3.4) along with the theoretical value. The deviation from the true value (solid line) is less then 0.1% for values of N greater then approximately 500 when the estimate of σ is based on E_F. An estimation based on E_D will typically give a deviation on the order of 10%, even for very large valued of N [2].

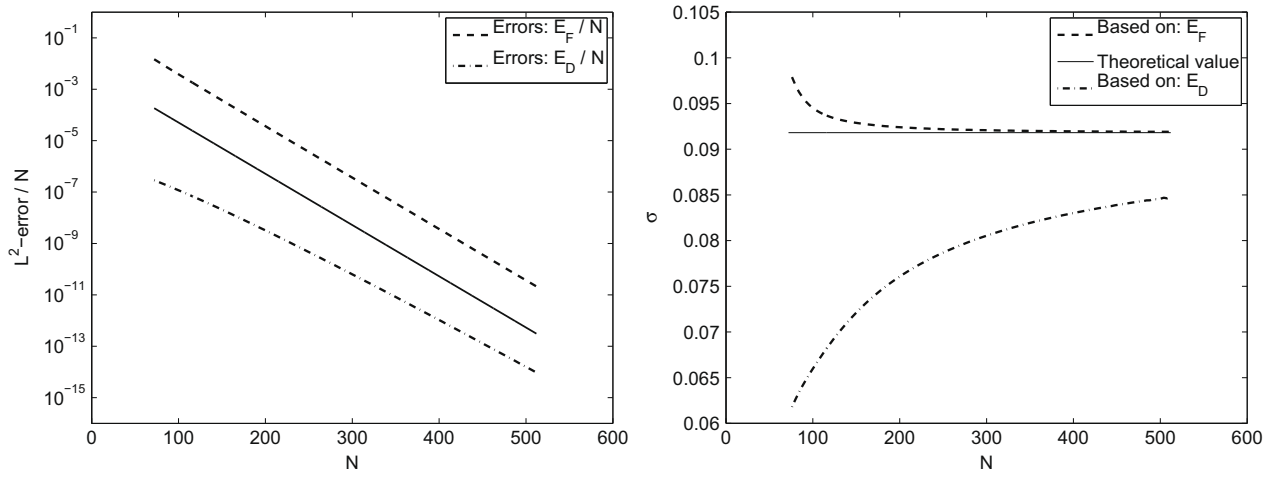

Fig. 2. Errors divided by N (left) and estimates of σ (right) after 10 time steps. The solid line in the left figure has slope $-\sigma$. The solid line in the right figure is the theoretical value of σ. Results are shown for $a = 34.2$, $\kappa = 0.5$ and $p = 2$.

The results for σ above depend on our assumption of the special form of the L^2-errors $E_F(N)$. The form used above is suggested by the convergence result in Theorem 2.2. However, the factor N could be of technical nature. Thus one might want to assume an alternative form of the dependence of the L^2-error on N. After some trial and error we have found a pattern for the assumed forms giving the most accurate estimates of σ in the special case of solitary wave solutions. These forms are suggested by

$$E_F(N) = \Lambda N^{-\frac{p-3}{p-1}} e^{-\sigma N} \tag{3.5}$$

for different values of p. In Table 1 we have summarized the results for p between 2 and 4. Along with the deviations between the computed and true values of σ, we have also recorded the sum of squares of residuals (SSR) in the different cases. The SSR value is an indication on how well the assumed form matches the data, and we see that there is a correspondence between this value and the deviation. The SSR value can thus be used as a tool when deciding between different alternative forms of the dependence of the L^2-error on N. An obvious form for the modulus of the large wavenumbers follows from the exact formulation of $\widehat{\Phi}_2(k)$ given in (3.3), namely

$$\widehat{\Phi}_2(k) \sim C\frac{k}{e^{\frac{\pi k}{2\kappa a}} - e^{-\frac{\pi k}{2\kappa a}}} = Cke^{-\frac{\pi k}{2\kappa a}}\frac{1}{1-e^{-\frac{\pi k}{\kappa a}}}$$

This shows that $|\hat{u}(k)| \sim Cke^{-\sigma k}$, for k large. More generally, as noted for instance in [1], the asymptotic behavior of solitary waves for $p \geqslant 2$ is given by

$$\widehat{\Phi}_p(k) \sim C|k|^{-\frac{p-3}{p-1}} e^{-\frac{\pi k}{2\kappa a}}$$

which matches the formula (3.5).

Coming back to the method described by Sulem et al., we again look at the exact solution (3.2) in the case $p = 2$. The least squares fit is then made between this assumed form and data for each value of N (for illustrative purposes, one value of N is sufficient). Since it is the large wavenumber behavior which is of interest, the fit starts at some $k_{min}(> 0)$. And to avoid that the results is contaminated by round off errors, the fit ends at some k_{max} as explained in [23]. In Fig. 3 the results for this method are shown. In Fig. 3 (left) we have plotted the modulus of the FT for the largest $N = 512$ used. The dots mark the range of wavenumbers used in the least squares fit. The estimates of σ based on the FT are plotted in Fig. 3 (right) together

Table 1
The assumptions on the form of the L^2-error is given on the top line of Table 1. The sum of squares of residuals (SSR) and the deviation (in %) from the theoretical value is listed for different values of p in the columns. It is seen that the forms with the smallest SSR corresponds to the most accurate predictions of σ.

$E(N)$	$\Lambda N e^{-\sigma N}$		$\Lambda e^{-\sigma N}$		$\Lambda N^{-1/3} e^{-\sigma N}$	
p	SSR	Deviation	SSR	Deviation	SSR	Deviation
2	3.83×10^{-15}	0.13	1.09×10^{-12}	−4.76	2.01×10^{-12}	−6.39
3	2.60×10^{-11}	5.86	3.93×10^{-21}	−0.000016	3.09×10^{-12}	−1.95
4	1.96×10^{-10}	9.16	1.17×10^{-11}	2.23	5.14×10^{-14}	−0.07

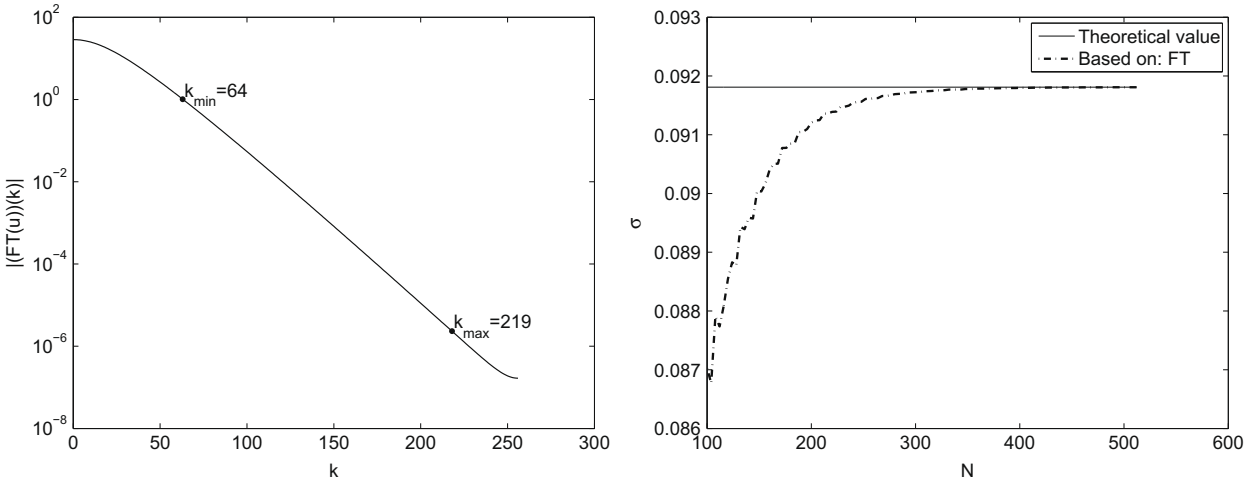

Fig. 3. The left figure show the modulus of the Fourier transform after 10 time steps for $N = 512$. The dots mark the range of wavenumbers used in the least squares fit for this particular value of N. Least squares fits for different N have produced the estimates of σ seen in the right figure. The solid line is the theoretical value of σ. Results are shown for $a = 34.2, \kappa = 0.5$ and $p = 2$.

with the theoretical value. The results are very accurate, and the deviation from the true value is less then 0.002% for the largest N.

The very accurate result for the latter method might be expected since an analytical expression for the FT of the solution is known in closed form and the assumed form for this really captures the large wavenumber behavior very well. With $N = 512$ the calculated SSR was approximately 5×10^{-8}. Furthermore, we have found that for different p the form of the modulus of the FT follows the same pattern as the L^2-errors for the special solitary wave solutions. Calculations as those leading to Table 1 for this second method, shows that the two different methods perform approximately equally well for $p = 3, 4$.

4. Radius of analyticity as a function of time

In the cases considered so far, the solutions do not change shape over time and, therefore, if the initial condition is a function in the space G_σ, the solutions will remain in G_σ for all time. Put another way, σ is constant in time. As intimated in Theorem 2.1, for general initial data, analytic in a strip in the complex plane, σ might change with time. For the generalized KdV equation, algebraic lower bounds of σ have been proved in [5]. The estimates in [5] provide a lower bound for the decrease of the radius of analyticity as a function of time. In particular, if $p = 2$ or $p = 3$, the estimates

$$\sigma(t) \geqslant Kt^{-12(p-1)} \tag{4.1}$$

hold true for some constant K, and for $t > 1$.

In the previous calculations, $E_F(N)$ was computed by comparing numerical and analytical solutions. For general initial data, these errors must instead be obtained by comparison with a high resolution numerical solution. Because of the exponential convergence rate this is not a serious drawback in practical terms. Runs done for the solitary waves after substituting the analytical expressions with a high resolution numerical solution, gave the same results as above.

Since the numerical experiments described in this section require long time integrations with high accuracy, a fourth-order time integration scheme is adapted to the problem. This scheme was proposed by De Frutos and Sanz-Serna in [12]. The method is based on the second order implicit midpoint rule. One step of the method uses the midpoint rule three times in succession, or in three stages, when advancing the solution in time. This method being implicit, it requires some iterations when solving the non-linear term. The linear stability analysis in [12] shows that the method is unconditionally stable on the whole imaginary axis. It is therefore well suited for integrating wave problems.

In order to compute σ as a function of time, a high resolution (high wavenumbers resolved to machine precision) numerical solution is calculated and stored at some given times. This is used as a reference when computing $E_F(N)$ for different resolutions N. Estimates of σ at the given times are then found as above. Estimates of σ in time using the method by Sulem et al. are obtained directly from the reference solution.

After experimenting with a wide set of initial data, it appeared that the decay rate (4.1) has not been achieved in any practical computation with the values $p = 2$ or $p = 3$. In fact, it appeared that all solutions were approaching a constant asymptotic value of σ for large t. This observation appears to be related to the fact the solutions of (1.1) are known to be bounded globally in time for $p \leqslant 4$. Fig. 4 (left) shows a typical output when σ is computed as a function of time. Although the curve jumps a bit about from one time to the next, the average of the time series of σ is approximately equal to σ at time $t = 0$. The initial data used was a positive bell-shaped hump given by $u_0 = 1/(1 + \tan h^2(ax)) - 1/2$, and in Fig. 4 (right) we have plotted the solution at the time $t = 300$.

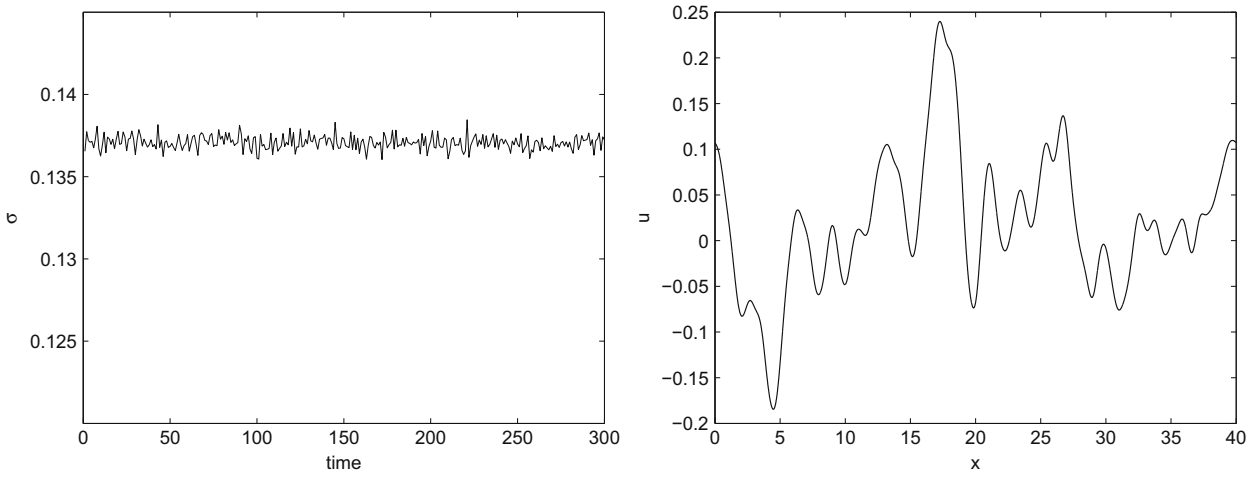

Fig. 4. The left figure shows σ computed as a function of time. The average value of $\sigma(t)$ is approximately equal to $\sigma(t = 0)$ for the initial data. The right figure shows the solution at time $t = 300$. Results are shown for $a = 6.37$ and $p = 2$.

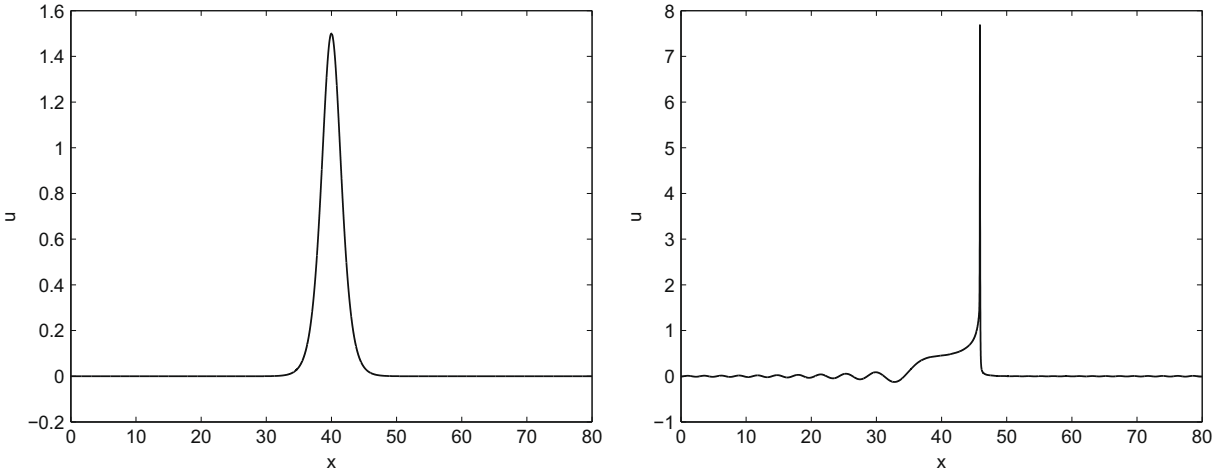

Fig. 5. The initial data (left) and the solution at $t = 2.0062$ close to the time of blow up (right). Results are shown for $a = 12.7$.

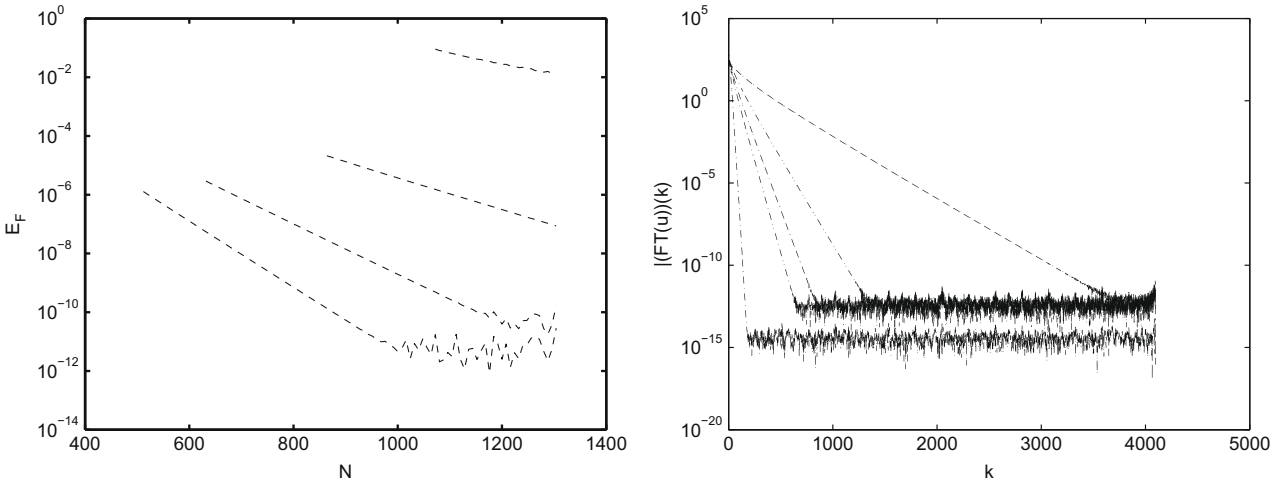

Fig. 6. The L^2-errors E_F (left) and the modulus of the Fourier transform (right) at times $t = 1$, 1.5, 1.875 and 2. In the right figure the modulus of the Fourier transform of the initial data are also shown. Results are shown for $a = 12.7$.

An altogether different picture emerged in the cases $p \geqslant 5$, where it is not known whether solutions are globally bounded. For initial data which are large enough in a certain sense, the solution may experience blow-up in finite time. Such a blow-up is characterized by a loss of regularity in the solution and a decrease of $\sigma(t)$ to zero. For the critical case $p = 5$, blow-up was suggested by asymptotic computations of Pelinovsky and Grimshaw [22], and indeed, blow-up has now been proved by Martel and Merle [21]. For $p \geqslant 5$, there are numerical studies of Bona, Dougalis, Karakashian and McKinney [3], indicating finite-time blow-up, and providing blow-up rates for certain norms. However, no proof of blow-up has been given so far for the cases $p > 5$.

Here, an experiment is set up for the case $p = 6$ in order to investigate how $\sigma(t)$ behaves up to around the time of blow-up of the solution. The initial and final data are shown in Fig. 5 (left) and Fig. 5 (right), respectively. Both methods for computing $\sigma(t)$ need a high resolution numerical solution. This is constructed as follows. A time step is chosen and the initial data are integrated giving solutions at certain times. These solutions are stored and the H^1-norms are calculated. Then, if the H^1-norm varies above a given tolerance from one time to the next, the time step is halved and the process repeated. The integration stops after the time step has been halved a given number of times or after a given number of iterations are reached. Using this reference solution the L^2-errors $E_F(N)$ can be calculated. A plot of these and the modulus of the FT of the (reference) solution at four different times are shown in Fig. 6. One problem with the method based on $E_F(N)$ when the solution eventually blows up, is that the numerical solutions with a moderate resolution N becomes unstable and breaks down before the actual time of blow up. Therefore quite large number of modes N are needed to compute the L^2-errors near this critical time. But at early times such relatively high resolution solutions are as accurate (to machine precision) as the reference and gives no information of the errors. Therefore, a wide range of resolutions are needed, and the solutions with low number of modes are eventually dropped as they break down when calculating the L^2-errors. This explains the graphs in Fig. 6 (left). These issues do not appear for the method of Sulem et al. which appears to be best suited for this type of investigation.

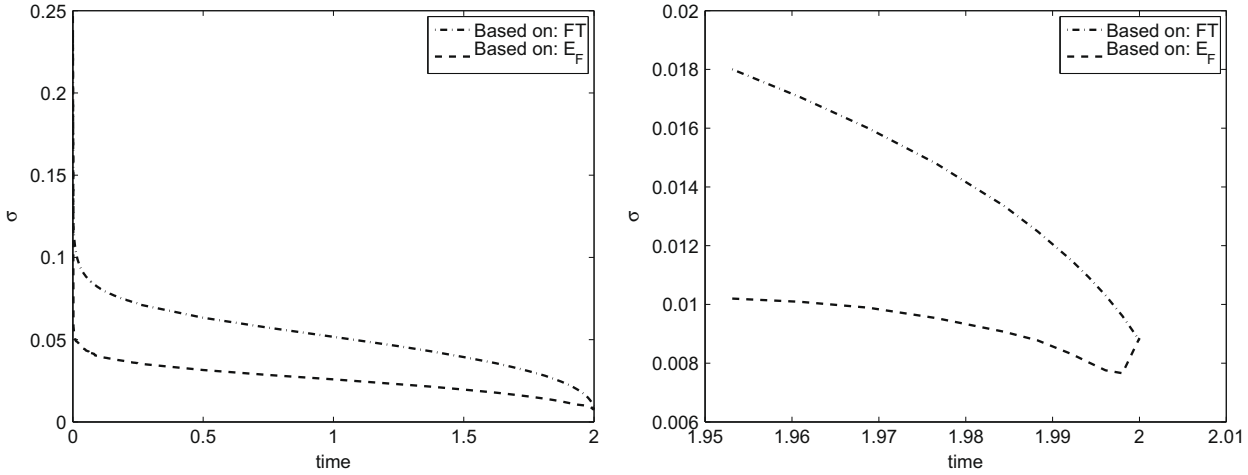

Fig. 7. In the left figure we have computed $\sigma(t)$ based on the Fourier transform (dashed-dotted line) and based on the L^2-errors (dashed line) in time. In the right figure a zoomed in version of the time around blow-up is shown. Results are shown for $a = 12.7$.

As can be seen in Fig. 7 (left), both methods show a rapid decay of $\sigma(t)$ at early times. This decay may be due to initial data splitting up into a small-amplitude solitary wave and an unstable, waveform featuring a large spike. At later times it is seen that $\sigma(t)$ decreases quite slowly, with the magnitude of $\sigma(t)$ somewhat larger for the method based on the FT. This difference gets smaller as one approaches the time of blow-up. Some time before this happens, however, we again see that $\sigma(t)$ starts to decrease quite rapidly. See Fig. 7 (right). This behavior seems intuitively appropriate for a solution featuring finite-time blow-up. But the $\sigma(t)$ computed from $E_F(N)$ actually increases in the region close to the suspected blow-up time, indicating that the method based on $E_F(N)$ is not as robust when very small values of $\sigma(t)$ are to be found.

In conclusion, it appears from our experiments that given initial data for equation (1.1) with $p \geqslant 6$, the outcome can be divided into two cases. Either the solutions stay bounded, and $\sigma(t)$ is bounded below by an absolute constant, or the solution blows up, and $\sigma(t)$ approaches zero. The first case resembles the behavior for $p < 5$, and generally occurs if the initial data are small enough. In the latter case, the method of Sulem et al. for estimating $\sigma(t)$ appears to be more robust. However, to accurately compute a solution featuring finite-time blow-up, it might be more advantageous to directly study the dynamics of the poles of a solution of (1.1) in the complex plane. For $p = 2$ and $\sigma(t) \geqslant c > 0$, such a study has been conducted in [10].

Acknowledgments

This paper was written while the second author was participating in the international research program on Nonlinear Partial Differential Equations at the Centre for Advanced Study at the Norwegian Academy of Science and Letters in Oslo during the academic year 2008/2009. The authors wish to thank Jerry L. Bona and Zoran Grujić for enlightening conversations. Support of the Research Council of Norway is also gratefully acknowledged.

References

[1] Birnir B, Ponce G, Svanstedt N. The local ill-posedness of the modified KdV equation. Ann Inst Henri Poincaré 1996;13:529–35.
[2] Bjørkavåg M, Kalisch H. Exponential convergence of a spectral projection of the KdV equation. Phys Lett A 2007;365:278–83.
[3] Bona JL, Dougalis VA, Karakashian OA, McKinney WR. Conservative, high-order numerical schemes for the generalized Korteweg–de Vries equation. Philos Trans Roy Soc Lond A 1995;351:107–64.
[4] Bona JL, Grujić Z. Spatial analyticity for nonlinear waves. Math Models Method Appl Sci 2003;13:1–15.
[5] Bona JL, Grujić Z, Kalisch H. Algebraic lower bounds for the uniform radius of spatial analyticity for the generalized KdV equation. Ann Inst H Poincaré, Anal NonLinéaire 2005;22:783–97.
[6] Bourgain J. Fourier transform restriction phenomena for certain lattice subsets and applications to nonlinear evolution equations. GAFA 1993;3:107–56. 209–62.
[7] Canuto C, Hussaini MY, Quarteroni A, Zang TA. Spectral methods in fluid dynamics. Berlin: Springer; 1988.
[8] Colliander J, Keel M, Staffilani G, Takaoka H, Tao T. Multi-linear estimates for periodic KdV equations, and applications. J Funct Anal 2004;211:173–218.
[9] Crighton DG. Applications of KdV. Acta Appl Math 1995;39:39–67.
[10] Deconinck B, Segur H. Pole dynamics for elliptic solutions of the Korteweg–de Vries equation. Math Phys Anal Geom 2000;3:49–74.
[11] Drazin PG, Johnson RS. Solitons: an introduction. Cambridge texts in applied mathematics. Cambridge: Cambridge University Press; 1989.
[12] De Frutos J, Sanz-Serna JM. An easily implementable fourth-order method for the time integration of wave problems. J Comput Phys 1992;103:160–8.
[13] Gorsky J, Himonas AA. Construction of non-analytic solutions for the generalized KdV equation. J Math Anal Appl 2005;303:522–9.
[14] Grujić Z, Kalisch H. Local well-posedness of the generalized Korteweg–de Vries equation in spaces of analytic functions. Diff Integral Eq 2002;15:1325–34.
[15] Kalisch H. Rapid convergence of a Galerkin projection of the KdV equation. CR Math 2005;341:457–60.
[16] Kalisch H, Raynaud X. Convergence of a spectral projection of the Camassa–Holm equation. Num Meth Partial Differ Eq 2006;22:1197–215.
[17] Kalisch H, Raynaud X. On the rate of convergence of a collocation projection of the KdV equation. M2AN Math Model Numer Anal 2007;41:95–110.
[18] Kato T, Masuda K. Nonlinear evolution equations and analyticity I. Ann Inst Henri Poincaré, Anal NonLinéaire 1986;3:455–67.
[19] E Kenig C, Ponce G, Vega L. A bilinear estimate with applications to the KdV equation. J Am Math Soc 1996;9:573–603.

[20] Maday Y, Quarteroni A. Error analysis for spectral approximation of the Korteweg–de Vries equation. RAIRO Model Math Anal Numer 1988;22:499–529.
[21] Martel Y, Merle F. Blow up in finite time and dynamics of blow up solutions for the L^2-critical generalized KdV equation. J Am Math Soc 2002;15:617–64.
[22] Pelinovsky DE, Grimshaw RHJ. An asymptotic approach to solitary wave instability and critical collapse in long-wave KdV-type evolution equations. Physica D 1996;98:139–55.
[23] Sulem C, Sulem P-L, Frisch H. Tracing complex singularities with spectral methods. J Comput Phys 1983;55:138–61.